Glacier mass and area changes on the Kenai Peninsula, Alaska, 1986-2016

Ruitang Yang[1,2,4], Regine Hock[2], Shichang Kang[1,3,4], Donghui Shangguan[1], Wanqin Guo[1]

[1]State Key Laboratory of Cryospheric Science, Northwest Institute of Eco-Environment and Resources, Chinese Academy of Sciences, Lanzhou 730000, China
[2]Geophysical Institute, University of Alaska Fairbanks, Fairbanks, AK, USA
[3]CAS Center for Excellence in Tibetan Plateau Earth Sciences, Chinese Academy of Sciences, Beijing 100101, China
[4]University of Chinese Academy of Sciences, Beijing 100049, China

Correspondence: Wanqin Guo <guowq@lzb.ac.cn >

Supplementary Tables

Supplementary Figures

Supplementary text

Table S1. Characteristics of eight NOAA climate stations (https://gis.ncdc.noaa.gov/maps/ncei/summaries/monthly) and one USGS station (Wolverine weather station) (https://www2.usgs.gov/landresources/lcs/glacierstudies/wolverine.asp) on the Kenai Peninsula used in this study. *ID* refers to the label used in Figure 1. *ID_source* is the identification used by NOAA, or in case of A4 by USGS. *Data coverage* refers to the total period of time when data are available for the period of record. All stations are part of the Global Historical Climatology Network.

ID	Name	ID_source	Latitude °	Longitude °	Elevation m a.s.l.	Period of record	Data coverage %
A1	Kenai Municipal Airport	USW00026523	60.58	-151.24	27.7	1899-2019	70
A2	Homer Airport	USW00025507	59.64	-151.49	19.5	1932-2019	97
A3	Seward Airport	USW00026438	60.13	-149.42	6.7	1908-2019	93
A4	Wolverine	USGS15236895	60.38	148.92	990	1967-2019	100
B1	Portage Glacier Visitor Center	USW00026492	60.79	-148.84	31.4	1998-2019	100
B2	Grouse Creek Divide	USS0049L14S	60.26	-149.34	213.4	1988-2019	94
B3	Harding Icefield	USR0000AHAR	60.15	-149.80	1280.2	2004-2019	94
B4	Middle Fork Bradley	USS0050K05S	59.78	-150.76	701	1990-2019	89
B5	Kachemak Creek	USS0050K07S	59.73	-150.66	506	2004-2019	99

Table S2. Data used to derive glacier outlines for years 1986, 1995, 2005 and 2016. The main images used are marked in bold.

Date	Sensor	Path/Row	Resolution m	Product ID
12 September 1986	**Landsat5 TM**	**69/18**	**30**	**LT50690181986255XXX05**
14 September 1986	**Landsat5 TM**	**67/18**	**30**	**LT05_L1TP_067018_19860914_20161003_01_T1**
20 August 1995	**Landsat5 TM**	**69/18**	**30**	**LT05_L1TP_069018_19950820_20160926_01_T1**
04 August 1995	Landsat5 TM	69/18	30	LT05_L1TP_069018_19950804_20160926_01_T1
26 September 1999	**Landsat7 ETM+**	**67/18**	**30**	**LE07_L1TP_067018_19990926_20161003_01_T1**
08 August 2005	**Landsat5 TM**	**68/18**	**30**	**LT05_L1TP_068018_20050808_20160912_01_T1**
08 September 2005	Landsat7 ETM+	69/18	30	LE70690182005251EDC00
09 August 2005	ASTER L1T	-	15	AST_L1T_003_08092005211851_20150510164811_78788
31 August 2016	**Landsat8 OLI**	**67/18**	**30/15**	**LC08_L1TP_067018_20160831_20170222_01_T1**
31 August 2016	Sentinel-2	-	10	S2A_OPER_MSI_L1C_TL_SGS__20160831T232504_A006232_T05VPG
03 August 2015	Landsat7 ETM+	69/18	30	LE70690182015215EDC00
11 August 2015	Landsat8 OLI	69/18	30/15	LC80690182015223LGN00

Table S3. Overview of the geospatial data sets (ASTER, ICESat, and IFSAR DEM) used in this study for glacier surface elevation change. Domain numbers refer to the subregions shown in Figure 1.

Date	Data source	Resolution m	Product ID	Domain	Image ID
09 August 2005	ASTER L1A	15	AST_L1A_00308092005211833_20171109192553_3427	IV, III	AST-4
14 August 2005	ASTER L1A		AST_L1A_00308142005213703_20171109192543_2864	II	AST-2a
14 August 2005	ASTER L1A		AST_L1A_00308142005213712_20171109192543_2863	I, II	AST-1
09 August 2005	ASTER L1A		AST_L1A_00308092005211842_20171204194210_1847	II, III	AST-2b
29 August to 12 September 2014	IFSAR DSM	5	USGS NED Digital Surface Model AK Kenai-Ifsar-L3-c309 2014	I, II	IFSAR DEM
	IFSAR DSM		USGS NED Digital Surface Model AK IFSAR-Chugach-c281 2016	II, III, IV	IFSAR DEM
	IFSAR DSM		USGS NED Digital Surface Model AK Kenai-L2-c280 2014	II	IFSAR DEM
	IFSAR DSM		USGS NED Digital Surface Model AK Kenai-L3-c310 2014	II	IFSAR DEM
	IFSAR DSM		USGS NED Digital Surface Model AK IFSAR-Chugach-c282 2016	III, IV	IFSAR DEM
	IFSAR DSM		USGS NED Digital Surface Model AK IFSAR-Chugach2-C308 2014	I	IFSAR DEM
	IFSAR DSM		USGS NED Digital Surface Model AK IFSAR-Chugach-c311 2016	III	IFSAR DEM
2003-2009	ICESat GLAH14_634	70	GLAS/ICESat L2 Global Land Surface Altimetry Data (HDF5) V034 (133 scenes)	I, II, III, IV	ICESat

Table S4. Vertical accuracy assessment of the IFSAR DEM for the Kenai Peninsula based on ICESat data. *N* is the number of ICESat points over stable terrain for different slope ranges, Δh is the mean difference between ICESat points and IFSAR DEM.

Slope	N	Δh	Standard deviation
		m	m
0°— 5°	767	0.53	1.38
5°— 10°	225	0.49	1.99
10°— 20°	261	0.78	2.66
20°— 30°	127	1.17	2.76
All	1380	0.63	1.94

Table S5. Model parameters and values used in the mass-balance model to compute the mass change between 11 August and 6 September 2005 to correct for the difference in acquisition dates between the ASTER (9 August and 14 August 2005) and IFSAR DEM (29 August - 12 September 2014). The model was run perturbing the parameters given in the column 'Value' with values within the specified ranges.

Parameter	Unit	Value	Range
Temperature bias*	℃		-0.5 to 0.5
Precipitation correction*	mm		-10% to 10%
Temperature lapse rate	℃ km^{-1}	-6.5	-0.05 to 0.05
Precipitation lapse rate	$mm\ (100\ m)^{-1}$	-	0 to 10
Elevation for firn line	m a.s.l.	1284 **	-100 to 100
Degree-day factor (snow)	$mm\ w.e.$ ℃$^{-1}$	-3.8***	-1 to 1
Degree-day factor (ice)	$mm\ w.e.$ ℃$^{-1}$	-4.7***	-1 to 1

* Daily air temperatures and precipitation from the Wolverine weather station (990 m a.s.l.) were perturbed by values within the specified range

** Assumed to correspond to the average ELA of Wolverine glacier over the period 1948-2018 (Baker and others, 2018)

*** Adopted from values derived for Wolverine glacier by O'Neel and others (2019)

Table S6. Uncertainty related to the residual elevation error over the stable terrain after co-registration (σ_{coreg}), for each ASTER DEM used in this study. *N* refers to the number of ICESat points on stable terrain, and *dz* is the summation of the vertical components of the 3D co-registration vectors (ASTER DEMs / IFSAR DEM /ICESAT).

Image ID	Domain	N	dz	σ_{coreg}	σ_{coreg}*
			m	m	m a^{-1}
AST-1	I, II	28	1.86	1.86	0.21
AST-2a	II	98	-2.13	2.13	0.24
AST-2b	II, III	68	1.47	1.47	0.16
AST-4	IV, III	55	1.14	1.14	0.13

*The residual vertical error per year is calculated by diving σ_{coreg} dividing 9 by the number of years (9) between 2005 and 2014.

Table S7. Linear trends in summer, winter air temperatures and winter precipitation at nine weather stations on the Kenai Peninsula (Fig. 1) for the period 1986-2016 and 2005-2016. Numbers in bold indicate that the changes are significant at $p<0.05$. Summer is May to September, while winter is October to April.

ID	Elevation m a.s.l.	Period	Air temperature ℃ $(10a)^{-1}$		Winter precipitation mm $(10\ a)^{-1}$
			Summer	Winter	
A1	28	1986-2016	**0.4**	0.4	**-45**
A2	20	1986-2016	0.2	0.3	-18
A3	7	1986-2016	0.1	0.03	-88
A4	990	1986-2016	0.2	-0.14	**-190**
B1	31	2005-2016	0.2	2.3	358
B2	213	2005-2016	0.1	1.6	200
B3	1280	2005-2016	0.2	**2.9**	—
B4	701	2005-2016	1.3	**4.9**	169
B5	506	2005-2016	**1.8**	**3.6**	362

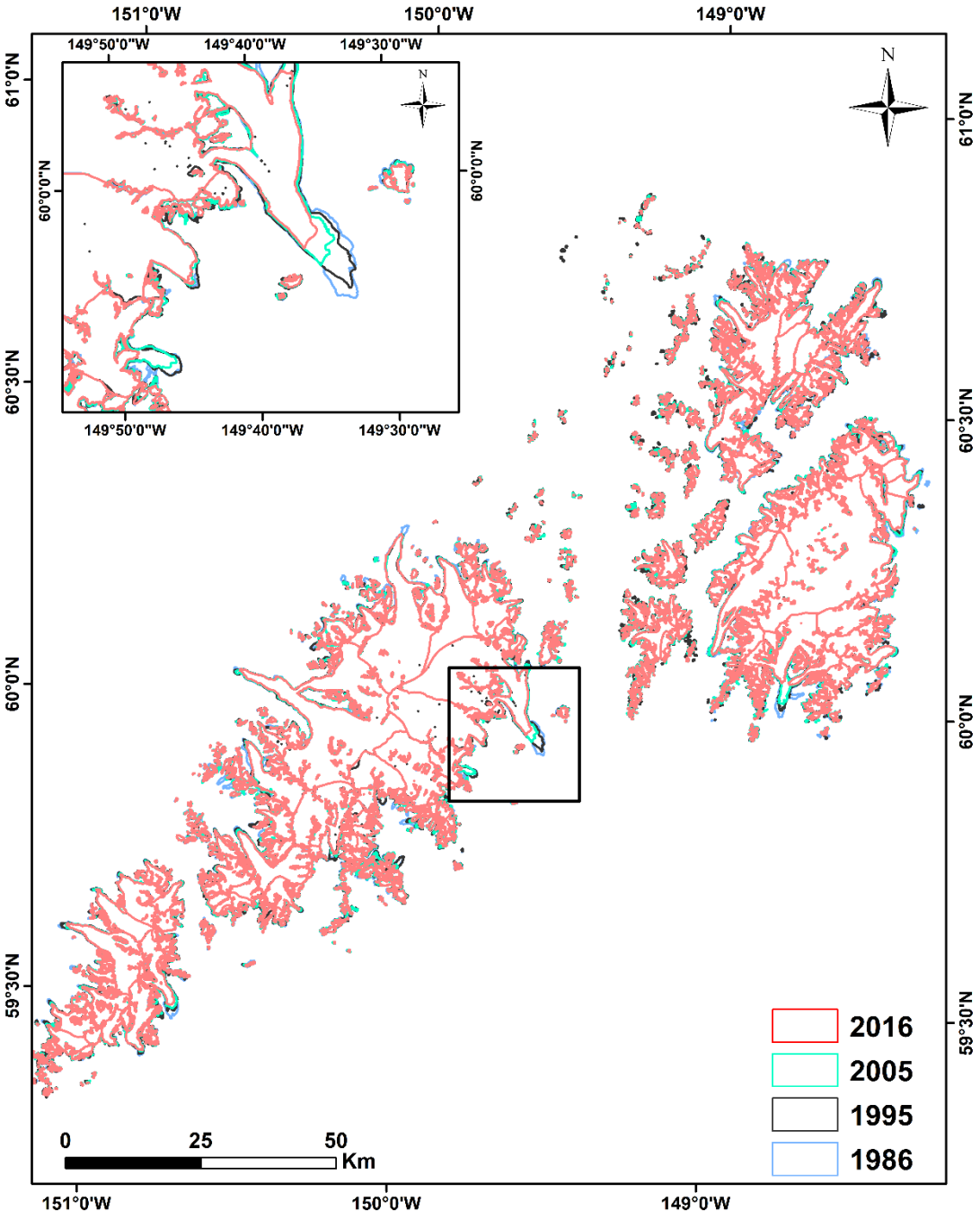

Fig. S1. Glacier outlines on the Kenai Peninsula in 1986, 1995, 2005, and 2016. The upper inset shows the outlines within the black rectangle.

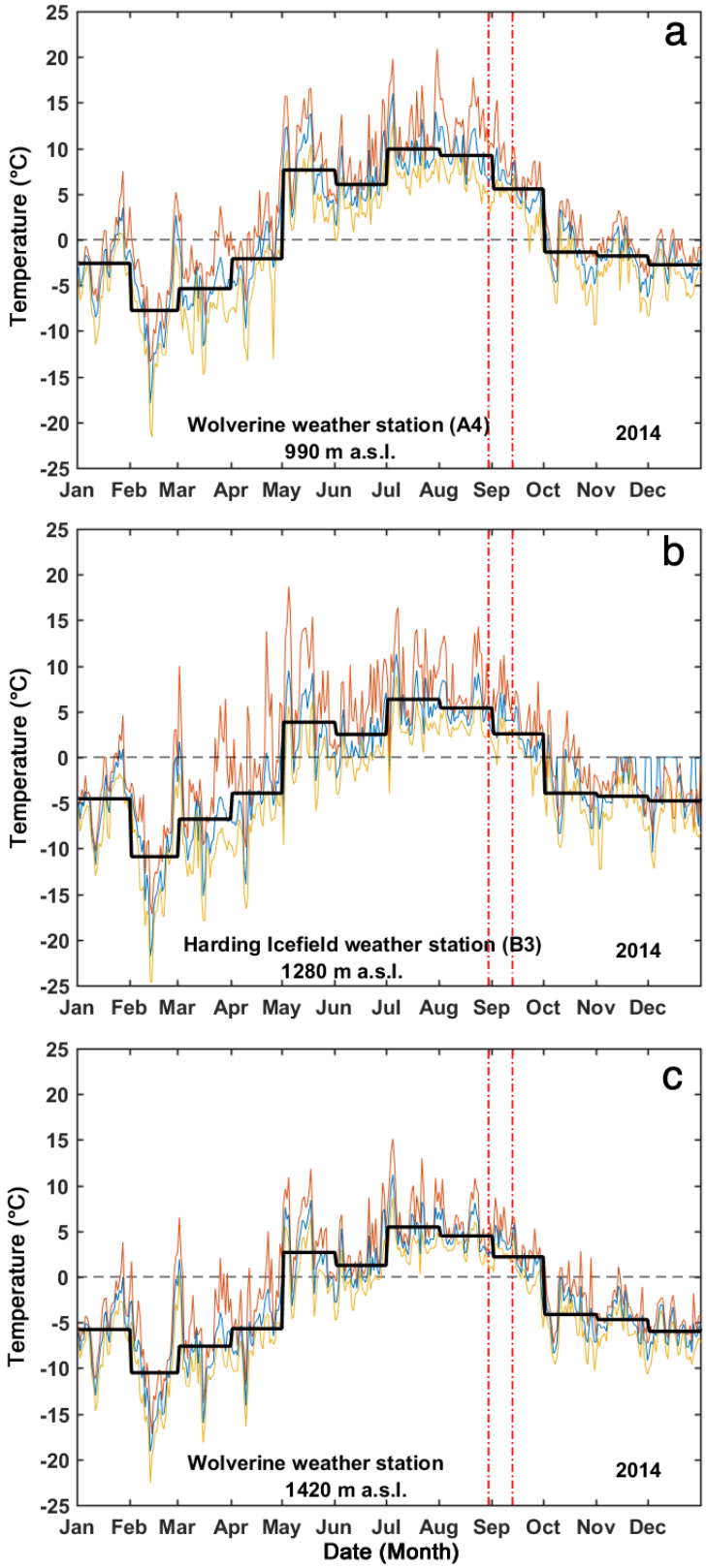

Fig. S2. Daily air temperature in 2014 from (a)Wolverine weather station (990 m a.s.l.), (b) Harding Icefield Field weather station (1280 m a.s.l.), and (c) Wolverine weather station (1420 m a.s.l.). See Fig.1 and Fig. S3 for locations. The dashed vertical lines mark the period 29 August to 12 September during which the source images of IFSAR DEM were acquired. The temperature data were used as an indicator of surface wetness to evaluate possible radar penetration.

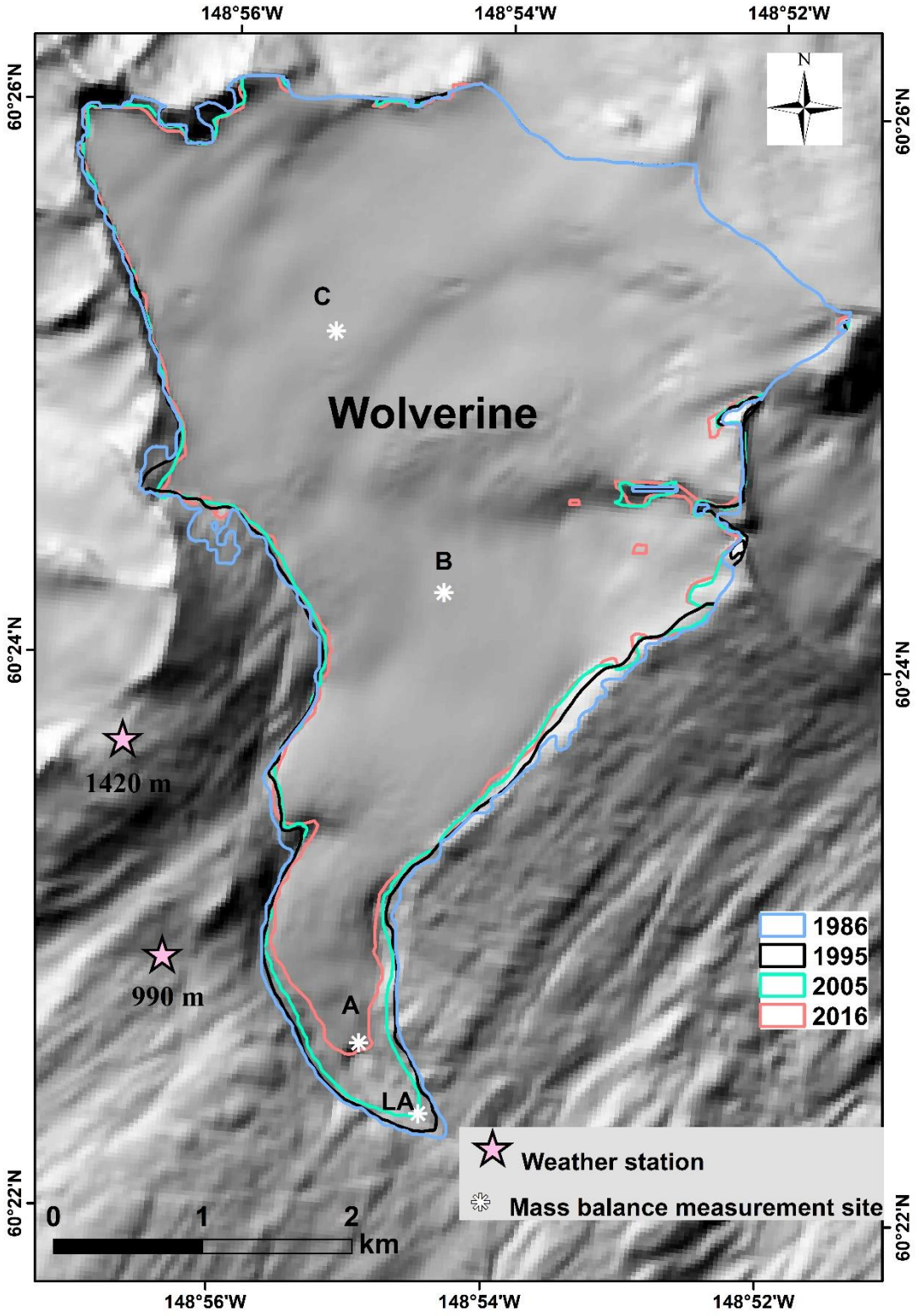

Fig. S3. Map of Wolverine glacier, with weather stations and mass-balance measurement sites labeled with site names. The colored polygons refer to glacier outlines in 1986, 1995, 2005 and 2016, respectively. The background is the hillshade of the IFSAR DEM.

Moving *t*-test technique

The moving *t*-test technique is used to test the difference in the mean of two sample populations of a random variable (Afifi and Azen, 1972). Here we used it to detect the possible abrupt change points by testing the difference between two subsamples before and after the change point with equal subsample size $n = n_1 = n_2$ (Fu and others, 1999). A sample x which is uncorrelated and normally distributed is defined over two subsamples x_1 and x_2, with the equal sample size n_i $(i = 1,2)$, the mean and variance μ_i and $\sigma_i (\mathrm{i} = 1,2)$. The null hypothesis H_0 is $\mu_1 = \mu_2$. The *t*-test statistic is estimated as follows:

$$t = \frac{\overline{x}_1 - \overline{x}_2}{s \cdot \sqrt{\frac{1}{n_1} + \frac{1}{n_2}}} \quad (1)$$

$$s = \sqrt{\frac{(n_1 - 1)s_1^2 + (n_2 - 1)s_2^2}{n_1 + n_2 - 2}} \quad (2)$$

where t is a ratio between the difference between the two groups and the difference within the groups, $\overline{x}_i$ $(i = 1,2)$ is the mean value of subsample $x_i (i = 1,2)$, s is the unbiased pooled sample standard deviation, n_i $(i = 1,2)$ is the number of degrees of freedom of each subsample, used in significance testing, while $n_1 + n_2 - 2$ is the total, $s_i^2 (i = 1,2)$ is the variance. The H_0 is rejected if $|t| > t_{\alpha,v}$, in which $t_{\alpha,v}$ is the quality of the Student's *t* distribution with the $n_1 + n_2 - 2$ degrees of freedom and α is the significance level of the test. Here, the moving *t*-test was used on sliding 5-year averages, $n_1 = n_2 = 5$ (Fig. S1).

References

Afifi, A.A. and Azen, S.P. (1972). Statistical Analysis, A Computer Oriented Approach, *Academic Press*, Harcourt Brace Jovanonich Publishers, New York, 366 pp.

Baker, E. H. and 9 others (2018), USGS Benchmark Glacier Mass Balance and Project Data: U.S.Geological Survey data release, https://doi.org/10.5066/F7BG2N8R

Fu C, Diaz HF, Dong D and Fletcher JO (1999) Changes in atmospheric circulation over northern hemisphere oceans associated with the rapid warming of the 1920s. I*nternational Journal of Climatology*, 19(6), 581-606, (doi: 10.1002/ (SICI) 1097-0088(199905)19:6<581: AID-joc396>3.0.CO; 2-P)

O'Neel S and 8 others (2019) Reanalysis of the US Geological Survey Benchmark Glaciers: long term insight into climate forcing of glacier mass balance. Journal of Glaciology, 65(253), 850-866 (doi:10.1017/jog.2019.66)